



HAL
open science

On the recirculation of ammonia-lithium nitrate in adiabatic absorbers for chillers

R. Ventas, A. Lecuona, Michel Legrand, M.C. Rodríguez-Hidalgo

► To cite this version:

R. Ventas, A. Lecuona, Michel Legrand, M.C. Rodríguez-Hidalgo. On the recirculation of ammonia-lithium nitrate in adiabatic absorbers for chillers. *Applied Thermal Engineering*, 2010, 30 (17-18), pp.2770. 10.1016/j.applthermaleng.2010.08.001 . hal-00678805

HAL Id: hal-00678805

<https://hal.science/hal-00678805>

Submitted on 14 Mar 2012

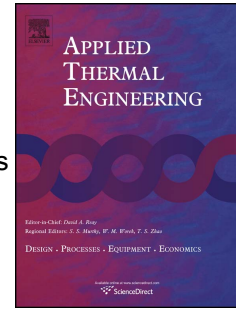
HAL is a multi-disciplinary open access archive for the deposit and dissemination of scientific research documents, whether they are published or not. The documents may come from teaching and research institutions in France or abroad, or from public or private research centers.

L'archive ouverte pluridisciplinaire **HAL**, est destinée au dépôt et à la diffusion de documents scientifiques de niveau recherche, publiés ou non, émanant des établissements d'enseignement et de recherche français ou étrangers, des laboratoires publics ou privés.

Accepted Manuscript

Title: On the recirculation of ammonia-lithium nitrate in adiabatic absorbers for chillers

Authors: R. Ventas, A. Lecuona, M. Legrand, M.C. Rodríguez-Hidalgo



PII: S1359-4311(10)00317-0

DOI: [10.1016/j.applthermaleng.2010.08.001](https://doi.org/10.1016/j.applthermaleng.2010.08.001)

Reference: ATE 3193

To appear in: *Applied Thermal Engineering*

Received Date: 5 April 2010

Revised Date: 22 July 2010

Accepted Date: 3 August 2010

Please cite this article as: R. Ventas, A. Lecuona, M. Legrand, M.C. Rodríguez-Hidalgo. On the recirculation of ammonia-lithium nitrate in adiabatic absorbers for chillers, *Applied Thermal Engineering* (2010), doi: [10.1016/j.applthermaleng.2010.08.001](https://doi.org/10.1016/j.applthermaleng.2010.08.001)

This is a PDF file of an unedited manuscript that has been accepted for publication. As a service to our customers we are providing this early version of the manuscript. The manuscript will undergo copyediting, typesetting, and review of the resulting proof before it is published in its final form. Please note that during the production process errors may be discovered which could affect the content, and all legal disclaimers that apply to the journal pertain.

1 On the recirculation of ammonia-lithium nitrate in adiabatic
2 absorbers for chillers

3
4 Ventas* R., Lecuona A., Legrand M., Rodríguez-Hidalgo M. C.

5
6 Departamento de Ingeniería Térmica y de Fluidos, Universidad Carlos III de Madrid,
7 Avda. Universidad 30, 28911 Leganés, Madrid, Spain, rventas@ing.uc3m.es

8
9
10 **Abstract**

11
12 This paper presents a numerical model of single-effect absorption cycles with ammonia-
13 lithium nitrate solution as the working pair and incorporating an adiabatic absorber. It is
14 based on $UA-\Delta T_m$ models for separate regions of plate-type heat exchangers and it
15 assumes an approach factor to adiabatic equilibrium. The results are offered as a
16 function of external temperatures. A loop circuit with a heat exchanger upstream the
17 absorber produces subcooling for facilitating absorption process. The effect of the mass
18 flow rate recirculated through the absorber is studied. Results show a diminishing return
19 effect. The value at which the recirculation mass flow yields a reasonable performance
20 is between 4 and 6 times the solution mass flow. With a heat transfer area 6 times
21 smaller than with a conventional diabatic shell-and-tube type absorber, the adiabatic
22 absorber configured with a plate heat exchanger yields a 2% smaller maximum COP
23 and a 15-20 % smaller cooling power.

24
25 **Keywords:** Absorption chiller, ammonia-lithium nitrate, adiabatic absorber, mass flow
26 recirculation.

27
28 **Nomenclature**

29
30 A Heat transfer area, m^2

1	COP	Coefficient of performance
2	cr	Circulation ratio
3	D	Solution mass diffusivity, $m^2 s^{-1}$
4	d	Droplet diameter, m
5	F_{ad}	Approach factor to adiabatic equilibrium
6	F_d	Approach factor to diabatic equilibrium
7	$F_{d,max}$	Approach factor to maximum ammonia mass fraction diabatic equilibrium
8	$F_{d,dmax}$	Ratio of approach factor to diabatic equilibrium and approach factor to
9		maximum ammonia mass fraction diabatic equilibrium for the same cycle.
10	h	Specific enthalpy, $J kg^{-1}$
11	Le	Lewis number = thermal diffusivity/mass diffusivity
12	l	Path length
13	\dot{m}_r	Refrigerant mass flow rate, $kg s^{-1}$
14	\dot{m}_{rr}	Recirculated mass flow rate, $kg s^{-1}$
15	\dot{m}_5	Solution mass flow rate at absorber outlet, $kg s^{-1}$
16	\dot{m}_6	Solution mass flow rate pumped by the solution pump, $kg s^{-1}$
17	\dot{m}_8	Solution mass flow rate at generator outlet, $kg s^{-1}$
18	\dot{m}_{10}	Solution mass flow rate at absorber inlet, $kg s^{-1}$
19	P	Pressure, Pa
20	P_{inj}	Injection pressure, Pa
21	\dot{Q}	Thermal power, W
22	rr	Recirculation ratio
23	T	Temperature, $^{\circ}C$
24	T_c	Condensation temperature, $^{\circ}C$

1	T_e	Evaporation temperature, °C
2	t	Residence time, s
3	U	Global heat transfer coefficient, $\text{W m}^{-2} \text{K}^{-1}$
4	v	Droplet velocity, m s^{-1}
5	$\dot{W}_{p,rr}$	Recirculation pump power, W
6	$\dot{W}_{p,s}$	Solution pump power, W
7	$X_{eq,ad}$	Adiabatic equilibrium ammonia mass fraction, outlet of absorber
8	$X_{eq,d}$	Diabatic equilibrium ammonia mass fraction, outlet of absorber
9	$X_{eq,dmax}$	Maximum diabatic equilibrium ammonia mass fraction, outlet of absorber
10	X_5	Ammonia mass fraction, outlet of absorber
11	X_8	Ammonia mass fraction, outlet of generator
12	X_{10}	Ammonia mass fraction, inlet of absorber
13	ΔT_{ml}	Mean logarithmic temperature difference, °C
14	η_{hb}	Pump hydraulic efficiency
15	η_{mb}	Electro-mechanical pump motor efficiency
16	τ	Non-dimensional time
17		
18	Subscripts	
19	a	Absorber
20	ahx	Absorber heat exchanger (subcooler)
21	ad	Adiabatic
22	bo	Boiling
23	c	Condenser
24	col	Vapour cooling

1	<i>d</i>	Diabatic (non-adiabatic)
2	<i>e</i>	Evaporator
3	<i>eq</i>	Equilibrium conditions
4	<i>g</i>	Generator
5	<i>i</i>	Inlet
6	<i>r</i>	Refrigerant
7	<i>rr</i>	Recirculation
8	<i>s</i>	Solution
9	<i>shx</i>	Solution heat exchanger
10	<i>sub</i>	Subcooling
11	<i>sup</i>	Superheating
12	<i>tp</i>	Two-phase

13

14 **1. Introduction**

15 The absorber is currently the largest size element of absorption single-effect
16 machines due to transferring heat and mass at the same time [1]. The most common
17 type of this element is a falling film configuration, either along horizontal or vertical
18 tubes in a shell-and-tube arrangement. The main problem for these configurations is the
19 bad liquid distribution/surface wetting [2], hence losing efficiency in the absorption
20 process. A similar process is performed in spray and plate heat exchanger (PHE)
21 absorbers, as they rely on falling film diabatic absorption. Other types of absorbers are
22 bubble absorbers and spray adiabatic absorbers [3].

23 The adiabatic absorber separates the processes of heat and mass transfer. The heat
24 evacuation occurs in an external conventional single-phase heat exchanger, which
25 allows reducing its size and cost, as it can be a commercial model. Moreover, if the heat

1 exchanger is a plate-type one, the heat transfer area needed is around 30 % of the area of
2 an equal power shell-and-tube heat exchanger [4]. Therefore, the plate heat exchanger
3 technology with adiabatic absorber seems to be an enabling factor for reducing the size
4 of the absorber.

5 The cooling happens before the poor in refrigerant (herewith ammonia) solution
6 flow enters the adiabatic absorber, where an adiabatic mass transfer process takes place
7 [5]. Usually mass transfer limits the absorption rate [6], being the liquid molecular
8 diffusion the factor that controls the absorption process. In order to reduce the
9 penetration length of the absorbed vapour into the liquid, the solution is sprayed. When
10 the drops start absorbing vapour their temperature rises, slowing absorption rate. If the
11 absorber is long enough, the adiabatic equilibrium is reached at the outlet of the
12 absorber because of a large residence time. However, as the absorption heat is not
13 evacuated the usual diabatic (non-adiabatic) equilibrium cannot be reached inside this
14 single pass absorber [1]; instead the equilibrium is at a higher temperature, thus with
15 less refrigerant absorbed. For this reason, there is need of an external recirculation and
16 subcooling of poor solution, so that a continuous multiple pass configuration results.

17 Different authors, e.g. [7, 8, 9 and 10], have studied the adiabatic absorption process
18 theoretically. Few authors [6, 11] carried out experimental studies. The results on these
19 works support its potential.

20 $\text{H}_2\text{O-LiBr}$ and $\text{NH}_3\text{-H}_2\text{O}$ are the best-known working pairs for single-effect
21 absorption cycles [12]. $\text{H}_2\text{O-LiBr}$ is commonly employed for air-conditioning purposes
22 due to its overall favourable performance. For industrial refrigeration, $\text{NH}_3\text{-H}_2\text{O}$
23 solution is the most common working fluid. $\text{NH}_3\text{-LiNO}_3$ is a promising alternative that
24 has been studied by [13, 14 and 15], among others. Single-effect absorption using this
25 solution offers slightly higher coefficients of performance (*COP*) and a lower

1 investment cost and size than $\text{NH}_3\text{-H}_2\text{O}$, as it does not require a rectification tower, e.g.
2 [15] and [16]. Lower driving temperatures for similar cooling purposes were reported in
3 [16]. Theoretical studies about adiabatic absorption using this solution have been
4 carried out in the last years [9] and [10].

5 There are still no rules on the suitable ratio of recirculation mass flow to solution
6 mass flow rates (rr) in adiabatic absorbers. This work aims at showing the influence of
7 rr on the absorption efficiency itself and also on the performance of a single-effect
8 based absorption cycle, using the promising $\text{NH}_3\text{-LiNO}_3$ solution. Comparison with two
9 diabatic absorbers with saturated solution at their outlet is offered as a reference and
10 discussed in terms of efficiency, size and electricity consumption.

12 **2. Description of the single-effect absorption with adiabatic and diabatic absorbers**

14 Fig. 1 shows the cycle layout of an absorption cycle with the adiabatic absorber. The
15 rich in refrigerant solution exits the absorber and is divided into two flows, the
16 recirculated flow (\dot{m}_{rr}) returning to the absorber and the flow that goes to the generator
17 (\dot{m}_5). \dot{m}_5 is pumped (point 6 in the cycle) through the solution heat exchanger and
18 preheated by the poor solution that comes from the generator. The rich solution enters
19 the generator (7) where ammonia vapour is desorbed and removed from the solution.
20 Poor solution returns to the absorber through the solution heat exchanger (8-9) and
21 lowers its pressure through the solution expansion valve (9). Downstream the valve, the
22 poor solution mixes with the recirculated flow and is cooled through the absorber heat
23 exchanger (subcooler). Finally, this flow is sprayed through injectors into the absorber
24 plenum by the remaining overpressure. This facilitates the incorporation of ammonia
25 vapour into the liquid solution. Ammonia liquid is produced in the condenser (1-2) at

1 condenser pressure (P_c) and is expanded (2-3). At low pressure (P_e) ammonia enters the
 2 evaporator and produces cold. The resulting ammonia vapour (4) enters the adiabatic
 3 absorber where it is absorbed by the solution spray.

4 Fig. 2 shows the same scheme of the absorption cycle but now with the diabatic
 5 absorber, either single pass (no recirculation) or with recirculation. Now inside the
 6 diabatic absorber the heat and mass transfer occurs simultaneously. This cycle will
 7 serve to evaluate the differences with the adiabatic absorber. The differences in
 8 thermodynamic state would vanish if both cycles reach diabatic equilibrium at the exit
 9 of the absorber. This would happen with infinitely large absorption residence time (ideal
 10 absorption, thus reaching saturation) and eventually with the cooperation of
 11 recirculation.

13 **3. Model**

14 3.1. System of equations

15 The numerical model is based on the simultaneous resolution of mass and energy
 16 steady state balance equations in all the components for either of both cycles.
 17 Correlations of Infante Ferreira [17] are used for the solution thermodynamic properties.
 18 Mechanical and chemical equilibrium are assumed at the exit of the components,
 19 excepting the absorber, e.g. at generator outlet, saturation is imposed at condenser
 20 pressure $P_{eq}(X_8, T_8) = P_c$. Losses and irreversibilities are concentrated at discrete points.
 21 The model is explained in detail in [18]. Only the fundamental issues that are related to
 22 absorption processes will be presented here.

23 For both cycles, solution and refrigerant mass balances in the generator are:

$$24 \quad \dot{m}_6 = \dot{m}_8 + \dot{m}_r \quad (1)$$

$$1 \quad \dot{m}_6 X_5 = \dot{m}_8 X_8 + \dot{m}_r \quad (2)$$

2 The recirculation and refrigerant mass balance for the adiabatic absorption cycle are:

$$3 \quad \dot{m}_{10} = \dot{m}_8 + \dot{m}_6 \cdot rr \quad (3)$$

$$4 \quad \dot{m}_{10} X_{10} = \dot{m}_8 X_8 + \dot{m}_6 \cdot rr \cdot X_5 \quad (4)$$

5 The recirculation ratio (rr) defines the mass flow recirculated towards the absorber
6 over the mass flow that goes to the generator, while circulation ratio (cr) refers to
7 solution mass flow pumped over the refrigerant flow:

$$8 \quad rr = \frac{\dot{m}_{rr}}{\dot{m}_6}; \quad cr = \frac{\dot{m}_6}{\dot{m}_r} \quad (5)$$

10 3.2. Absorption figures of merit

12 The approach factor to adiabatic equilibrium F_{ad} is the ratio of the change in mass
13 concentration achieved at the outlet of the adiabatic absorber spray plenum over the
14 change in concentration reaching adiabatic equilibrium:

$$15 \quad F_{ad} = \frac{X_5 - X_{10}}{X_{eq,ad} - X_{10}} \quad (6)$$

18 In order to illustrate the values of this figure of merit and to shed some light on its
19 dependence on the operative parameters some discussion follows. The collision
20 probability of the spray under conditions practical to absorption is very small, so that
21 independent droplet absorption is currently accepted, e. g. [9], [19] and [23].

22 F_{ad} , in other words the efficiency of the mass absorption process in respect to the
23 adiabatic equilibrium state, mainly depends on the diameter of the droplet (d), its
24 velocity (v) and the length of its flight inside the absorption plenum chamber (l), which
25 determines the residence time (t). Besides that, it depends on the diffusion coefficient of

1 ammonia in the solution (D), properties of the liquid and vapour phase, its turbulence
 2 intensity and Reynolds number in the liquid droplet, which determines the fluid motion
 3 inside the droplet. The droplet forming process and the external viscous flow shear
 4 causes it. This motion enhances absorption. If this phenomenon is neglected jointly with
 5 the external convection, a lower absorption rate results. Under this circumstance, a
 6 simple estimation of F_{ad} is obtained if homogeneous temperature is assumed inside a
 7 spherical droplet, which requires that the liquid Lewis number $Le \gg 1$, which is the
 8 case. The resulting equation for F_{ad} (Newman [19]) shows a growing value when the
 9 characteristic non-dimensional residence time τ (a mass transfer Fourier number) grows,
 10 so that for $\tau > 0.183 \Rightarrow F_{ad} > 0.9$:

$$11 \quad F_{ad} = 1 - \frac{6}{\pi^2} \sum_{i=1}^{\infty} \frac{\exp(-\pi^2 i^2 \tau)}{i^2}; \quad \tau = \frac{tD}{(d/2)^2} \quad (7)$$

12 Estimation of t is not straightforward owing to the varied trajectories the droplets
 13 will follow inside the plenum and the decelerating effect of the ammonia vapour. An
 14 even lower bound for F_{ad} is obtained if a constant velocity rectilinear trajectory is
 15 assumed, so that $t = l/v$. For order of magnitude estimation, taking $l = 0.2$ m, $v = 1$ m/s
 16 and $d = 300$ μm yields $F_{ad} = 0.63$, which still is an interesting figure. The mere
 17 inclusion of internal motion inside the droplet will lead to $F_{ad} = 0.85$, according to the
 18 Kronig and Brink model [23], which is expressed in similar terms as eq. (7). This
 19 indicates that including the rest of neglected phenomena and the residual absorption of
 20 the liquid film on the walls, according to theory a value for F_{ad} near unity would result
 21 in practice for this case. A selection of supporting studies on the topic is [19] to [23],
 22 indicating that even higher values are possible when the remaining parameters are
 23 considered. Both, experimental and numerical studies of exothermic adiabatic droplet
 24 absorption have been expressed in similar terms as the Newman equation, [6] and [11]

1 but using just the first ones of the series. Results of a numerical model fo film
 2 absorption [24] has showed that film absorption follows the same time evolution
 3 functional form than Newman model predicted for droplets.

4 Experimental results, offered below, corroborate the above considerations. As F_{ad}
 5 depends on complex thermo-fluid process of spray absorption, here it will be used as
 6 input variable not precising how it will be achieved, but being sure that values near
 7 unity are achievable.

8 The adiabatic equilibrium mass concentration $X_{eq,ad}$ is calculated at the constant
 9 pressure of the absorber P_e and at the higher adiabatic equilibrium temperature $T_{eq,ad}$,
 10 which comes from the following equation:

$$11 \quad P_{eq}(X_{eq,ad}, T_{eq,ad}) = P_e \quad (8)$$

12 The energy balance in the absorber for the case of reaching the adiabatic equilibrium
 13 is:

$$14 \quad \dot{m}_8 \cdot h_{10} + \dot{m}_{r,eq} \cdot h_4 = (\dot{m}_8 + \dot{m}_{r,eq}) h_{eq,ad} \quad (9)$$

$$15 \quad h_{eq,ad} = h_{eq}(X_{eq,ad}, T_{eq,ad}) \quad (10)$$

16 The corresponding refrigerant mass balance in the absorber is:

$$17 \quad \dot{m}_8 \cdot X_8 + \dot{m}_{r,eq} = (\dot{m}_8 + \dot{m}_{r,eq}) \cdot X_{eq,ad} \quad (11)$$

18 The approach factor to diabatic equilibrium F_d is used to compare the performance
 19 of the adiabatic absorber with what can be achieved in an equivalent diabatic absorber
 20 reaching saturation, thus ideal. This parameter is defined as the ratio of the change in
 21 refrigerant mass concentration achieved at the exit of the adiabatic absorber over the
 22 change in concentration reaching the diabatic equilibrium at the same pressure:

$$23 \quad F_d = \frac{X_5 - X_8}{X_{eq,d} - X_{8,d}} \quad (12)$$

1 The concentration at the outlet of the absorber that reaches saturation the diabatic
 2 equilibrium (in this sense ideal, *i.e.* involving the maximum X reachable with a finite
 3 value of UA) $X_{eq,d}$ is calculated modelling, the same way as before, an absorber in
 4 which the mass and heat transfer proceed inside the absorber, as shown in Fig. 2. This
 5 simulation is carried out with the same inlet parameters as the adiabatic absorber cycle,
 6 Table 1. This simulation was performed with a same finite value of heat conductance
 7 (UA_a) as the adiabatic absorber (UA_{ahx}), thus it is called “equivalent”. For this purpose,
 8 the mean logarithmic temperature difference at the diabatic absorber is defined as usual:

$$9 \quad \Delta Tlm_a = \frac{(T_{10} - T_{ao}) - (T_5 - T_{ai})}{\ln\left(\frac{(T_{10} - T_{ao})}{(T_5 - T_{ai})}\right)} \quad (13)$$

10 It is worth to note that diabatic equilibrium with finite heat conductance can be
 11 approached in practice with a high enough recirculation rate. Recirculation, indicated in
 12 Fig. 2, is common in large size absorption machines.

13 Still another reference is useful, again considering saturation at the exit of the
 14 diabatic absorber, but at the external circuit inlet temperature, what is common in cycle
 15 calculations [1], representing the maximum possible. The approach factor to the
 16 maximum ammonia mass fraction F_{dmax} considers reaching this diabatic equilibrium, as
 17 the reference. Therefore, it corresponds to the same eq. (12), but now using a
 18 conductance UA_a of infinite value, and infinite value for the external flow rate. As
 19 above indicated the temperature of equilibrium now coincides with the external inlet
 20 temperature to the absorber ($T_{a,i}$), usually named recooling inlet temperature:

$$21 \quad F_{dmax} = \frac{X_5 - X_8}{X_{eq,dmax} - X_{8,dmax}} \quad (14)$$

1 $F_{d,dmax}$ compares both diabatic absorbers considered, the equivalent one, and the one
 2 that reaches the maximum diabatic absorption at its outlet, so reaching the external
 3 circuit inlet temperature. Thus it is the ratio of F_{dmax} to F_d for the same fixed operating
 4 conditions, shown in Table 1.

$$5 \quad F_{d,dmax} = \frac{X_{eq,d} - X_{8,d}}{X_{eq,dmax} - X_{8,dmax}} \quad (15)$$

6 3.3. Cycle efficiency

7 The new mass concentration $X_{eq,dmax}$ comes from an equilibrium condition:

$$8 \quad P_{eq}(X_{eq,dmax}, T_{a,i}) = P_e \quad (16)$$

9 The coefficient of performance of the cycles is defined as follows:

$$10 \quad COP = \frac{\dot{Q}_e}{\dot{Q}_g} \quad (17)$$

11 The following equations allow calculating the electrical power consumptions of the
 12 solution pump and the recirculation pump:

$$13 \quad \dot{W}_{p,s} = \frac{\dot{m}_6 (P_c - P_e)}{\rho_5 \eta_m \cdot \eta_h} \quad (18)$$

$$14 \quad \dot{W}_{p,rr} = \frac{\dot{m}_{rr} (P_{inj} - P_e)}{\rho_5 \eta_m \cdot \eta_h} \quad (19)$$

15 3.4. Working conditions

16 Table 1 summarizes the input parameters to the cycle that are kept constant. All the
 17 characteristics of the external flows are input constants: inlet temperatures and mass
 18 flow rates as well as the characteristics of the heat exchangers, i.e., the global heat
 19 transfer coefficients U for each type of flow region (single or two-phase) and the total
 20 transfer areas, are input constants. As can be seen in Table 1, different values for U are
 21 taken for each phase region inside each heat exchanger and the corresponding area is

1 part of the system of equations solution, excepting the two alternative absorber heat
2 exchangers as they embrace a single region. Moreover, according to [18] energy and
3 mass balances at the saturation condition determine the surface area for each region
4 until phase change is complete. Downstream or upstream this boundary, surface area is
5 determined by the corresponding subcooling or superheating conditions and the total
6 prescribed heat transfer surface. This way the resulting equivalent U for the whole
7 exchanger allows matching the prescribed UA and the resulting total area A through the
8 system of equations. However, to compare the performance of the adiabatic cycle with
9 the diabatic one, the overall conductance of the absorber in the diabatic case was
10 calculated with the same value as the adiabatic one ($UA_{ahx} = UA_a$). Therefore, the input
11 variable for calculating both the diabatic absorber cycle performance was UA_a and not
12 U_a and A_a separately.

13 The model equations were numerically solved by means of the software EES[®], [25].

14

15 4. Results and discussion

16

17 Figure 3 shows the variation of COP with recirculation ratio rr for different values
18 of F_{ad} (considered as an input everywhere) and a representative but moderate hot
19 driving water temperature $T_{g,i} = 85$ °C. One can observe that when F_{ad} is increased the
20 COP rises for every rr because of the improvement on the ammonia absorption. The
21 lower the F_{ad} the higher are the differences between the curves. For each curve, when rr
22 increases, the value of COP rises, again as a result of the increased ammonia absorption.
23 For values of rr lower than about 4, for the case of $F_{ad} = 1$, the COP rises rapidly,
24 meanwhile for higher values the curves switch to a smaller slope. The switching point
25 rises slightly for lower F_{ad} .

1 The variation of the cooling capacity \dot{Q}_e with the recirculation ratio rr for different
 2 values of F_{ad} , again for $T_{g,i} = 85$ °C, is shown in Figure 4. \dot{Q}_e rises when F_{ad} and rr
 3 increase, similarly as commented for the COP curves, but with a higher sensitivity, as
 4 now more refrigerant absorption means a twofold improvement, more COP and more
 5 mass. For $F_{ad} = 1$ \dot{Q}_e rises rapidly up to $rr \approx 5$ meanwhile for higher values of rr \dot{Q}_e
 6 rises at a lower pace, but the change in slope is not such apparent as in Figure 3. When
 7 F_{ad} decreases the value for which the curves change in slope slightly decreases, in
 8 contrast with the case of the COP curves. \dot{Q}_e seems to continue rising significantly up
 9 to $rr \approx 10$.

10 Figure 5 shows the variation of the approach factor to diabatic equilibrium F_d and
 11 the approach factor to maximum ammonia mass fraction diabatic equilibrium $F_{d,max}$,
 12 with recirculation ratio rr , for different approach factors to adiabatic equilibrium F_{ad} ,
 13 again for $T_{g,i} = 85$ °C. Both F_d and $F_{d,max}$ rise with the increase of F_{ad} , being the rise
 14 higher for the curves of F_d . The maximum values are reached for the best possible value
 15 $F_{ad} = 1$ (adiabatic equilibrium). They were computed up to $rr = 10$ yielding $F_d = 0.8$ and
 16 $F_{d,max} = 0.64$. These values indicate that the adiabatic absorption efficiency is far from
 17 unity, the respective maxima possible, and that not much difference exists between F_d
 18 and $F_{d,max}$, respectively the diabatic saturated absorbers with equivalent UA and the one
 19 with $UA_a = \infty$. As already commented for \dot{Q}_e , the values where the curves switch their
 20 slope slightly decrease for lower rr .

21 Figure 6 shows the variation of the coefficient of performance COP with driving
 22 inlet temperature $T_{g,i}$ for different recirculation ratios rr and the best value possible:
 23 $F_{ad} = 1$ (adiabatic equilibrium) for the adiabatic and as a reference, the equivalent
 24 saturated diabatic absorption cycles. The COP curves rise when rr increases for all the

1 $T_{g,i}$ simulated. The differences between curves are slight for $rr = 4, 6$ and 8 , meanwhile
 2 for $rr = 0$ (single pass) the curve tendency is different from the others and the values are
 3 noticeably lower. The differences between curves decrease slightly with increasing $T_{g,i}$.
 4 The recirculation ratio that almost reaches the maximum COP is $rr \approx 4$. The maximum
 5 COP found for the highest recirculation ratio used, $rr = 8$, is close to the diabatic COP ,
 6 being 0.66 for the adiabatic absorber and 0.67 for the diabatic one, which represents less
 7 than 2% loss. It is worth to mention that these differences are lower with higher driving
 8 temperatures, as a result of the higher driving force for absorption. Figure 7 shows the
 9 variation of cooling capacity \dot{Q}_e with driving inlet temperature $T_{g,i}$ for different
 10 recirculation ratios rr and again $F_{ad} = 1$. This figure also shows \dot{Q}_e for the cycle with
 11 equivalent diabatic absorber. The curves rise almost linearly with the increase of $T_{g,i}$.
 12 Thus indicating that neither evaporator overflow nor condenser insufficient
 13 condensation appears, according to [18]. The figure depicts a higher cooling capacity
 14 \dot{Q}_e for a higher rr , decreasing the differences between curves for the highest values of rr .
 15 In contrast with the COP curves the differences between curves herewith enlarge with
 16 the increase of $T_{g,i}$, as well as the differences between $rr = 4$ and $rr = 8$ are larger. \dot{Q}_e
 17 for $rr = 6$ is almost the maximum, so the increase of rr above $rr = 6$ does not
 18 substantially improve the cooling capacity. The differences between the maximum
 19 recirculation ratio considered, $rr = 8$, and the diabatic cycle grow with $T_{g,i}$, but the
 20 proportion diminishes, being the adiabatic cooling power 20% lower at $T_{g,i} = 90\text{ }^\circ\text{C}$ and
 21 a mere 15% lower at $T_{g,i} = 110\text{ }^\circ\text{C}$.

22 Table 2 shows the values of the enthalpy, temperature and concentrations at the inlet
 23 and outlet of the absorber for the cases of the adiabatic absorber with $rr = 0$ and $rr = 6$,
 24 for $F_{ad} = 1$ and the equivalent diabatic absorber cycle for $T_{g,i} = 85\text{ }^\circ\text{C}$.

1 Figure 8 shows the variation of F_d and F_{dmax} with $T_{g,i}$, for different recirculation
 2 ratios rr and as before, $F_{ad} = 1$. All the curves grow with the increase of $T_{g,i}$, rapidly for
 3 low driving temperatures and slower for higher one's. This rise is greater for F_d than for
 4 F_{dmax} , especially for high rr values, indicating that high $T_{g,i}$ is especially in favour of the
 5 adiabatic absorber approaching the equivalent diabatic absorber performance. As the
 6 curves show, the values for $rr = 6$ and $rr = 8$ are very close together for all the $T_{g,i}$
 7 simulated, suggesting that an increase above 8 does not much improve the performance
 8 of the adiabatic absorber. The range of values of F_d for $rr = 8$ from $T_{g,i} = 85$ °C to
 9 122 °C, whereas the machine will likely operate, is from 0.74 to 0.88, meanwhile the
 10 range of values of F_{dmax} is from 0.62 to 0.65. This difference increases with an increase
 11 in $T_{g,i}$, as Figure 8 shows, as a consequence of higher heat power evacuated through
 12 UA_a . Figure 8 shows too the above defined parameter $F_{d,dmax}$. The results indicate that
 13 with conventional diabatic absorbers, a loss in absorption efficiency has to be accepted
 14 owing to finite heat conductance, similarly to what has been described for adiabatic
 15 absorbers.

16 The variation of F_d with driving inlet temperature $T_{g,i}$ for different absorber heat
 17 exchanger conductances UA_{ahx} is shown in Figure 9. Again $F_{ad} = 1$ has been chosen to
 18 isolate the effect of heat transfer conductance and solution thermodynamics from mass
 19 transfer conductance. The increase of UA_{ahx} improves F_d , but the improvement is more
 20 important for the smallest values of UA_{ahx} considered. This growth approaches the
 21 performance of the adiabatic absorber to the diabatic equivalent one.

22 The increase of UA_{ahx} in the adiabatic absorption cycle does not mean that this heat
 23 exchanger is larger than the diabatic absorber. As explained in the introduction, the
 24 falling film configuration is the most common for diabatic absorbers and they use to
 25 rely on a shell-and-tube type heat exchanger. In [4] it is commented that the heat

1 transfer area for an equal power plate heat exchanger is 30 % of a shell-and-tube heat
2 exchanger. In addition to that, in [2] Jeong and Garimella comment that the wetted
3 surface in a falling film absorber can be around 50 % of the total available. This means
4 that the heat transfer area, for the same conductance, with the diabatic shell-and-tube
5 absorber can be more than 6 times larger than with a plate type one. Nevertheless, to
6 compare both absorber types on a fair basis it is necessary to consider also the adiabatic
7 absorber plenum size. The plenum height of a spray absorber needed to reach $F_{ad} = 0.8$
8 with $\text{LiNO}_3\text{-NH}_3$ as working fluid is around 205 mm. This has been found
9 experimentally, [26], for a solution mass flow rate ranging between 0.041-0.083 kg/s,
10 relying on 7 commercial swirl pressure injectors of the fog type, nominally producing
11 an average droplet diameter of $d = 310 \mu\text{m}$. This means that the adiabatic absorber does
12 not eliminate the size advantage so far, neither signifies a substantial cost overrun. The
13 consequence is that the total area and volume saved with the adiabatic absorber can be
14 quite significant.

15 The recirculation pump power $\dot{W}_{p,rr}$, is obtained using eq. (17) and the experimental
16 data available in [26], being $P_{inj}-P_a = 1.5 \times 10^5 \text{ Pa}$. The results are $\dot{W}_{p,rr} = 231 \text{ W}$ for $rr =$
17 8 and the solution pump power $\dot{W}_{p,s} = 216 \text{ W}$, eq. (16), both for a nominal capacity $\dot{Q}_e =$
18 4 kW at $T_{g,i} = 85 \text{ }^\circ\text{C}$.

19

20 5. Conclusions

21

22 Detailed models for a single-effect absorption cycle with an adiabatic absorber and
23 both a diabatic saturated equivalent and an ideal absorber have been implemented using

1 the $\text{NH}_3\text{-LiNO}_3$ solution. The following conclusions can be drawn from the present
2 study:

3 - Saturation at the external recooling temperature is not reached neither
4 with adiabatic nor diabatic absorber with finite absorber heat conductance, even
5 in the case of equilibrium complete absorption (saturation), affecting both the
6 COP and the cooling capacity \dot{Q}_e .

7 - The recirculation loop is necessary in adiabatic absorbers for the cycle to
8 operate with a reasonable performance.

9 - For operating conditions leading to a reasonably high value of COP , this
10 parameter is less sensitive to recirculation ratio rr than the cooling capacity \dot{Q}_e .

11 - The recirculation ratio to almost reach the maximum performance for
12 adiabatic absorbers could be found to be between $rr = 4$ and $rr = 6$.

13 - For the same heat conductance UA_a the adiabatic absorber offers almost
14 the same COP figures as a complete absorption diabatic absorber, but with 15-20
15 % lower cooling capacity, at the maximum recirculation explored $rr = 8$.

16 - The size of the absorber subcooler in the adiabatic arrangement could be
17 down to 6 times smaller than with the diabatic arrangement and the plenum size
18 is not excessive. The price to pay is an extra pump, being its electricity
19 consumption almost the same than the solution pump.

20 - An increase of the subcooler heat conductance UA_{ahx} , for the adiabatic
21 absorber, improves the performance of the cycle, but at the expense of a minor
22 size reduction.

23

1 Acknowledgements

2 The financial support of this study by the Spanish Ministry of Education and
3 Science research grant ENE2005-08255-C02-02 and Project CCG07-UC3M/ENE-3411,
4 financed by the Local Government of Madrid and UC3M, are greatly appreciated.

5

6 References

7

- 8 [1] K. E. Herold, R. Radermacher, S. A. Klein. Absorption chillers and heat pumps,
9 CRC Press, 1996.
- 10 [2] S. Jeong, S. Garimella. Falling-film and droplet heat transfer in a horizontal tube
11 LiBr/water absorber. International Journal of Heat and Mass Transfer, 45 (2002)
12 1445-1458.
- 13 [3] M. Venegas. Transferencia de masa y calor en gotas en procesos de absorción con
14 nitrato de litio-amoniaco: Nuevas tecnologías. PhD Thesis, Universidad Carlos III
15 de Madrid, 2002.
- 16 [4] L. Wang, B. Sunden, R.M. Manglik. Plate heat exchangers. Design, applications
17 and performance, Wit Press, 2007.
- 18 [5] F. Flamensbeck, F. Summerer, P. Riesch, F. Ziegler, G. Alefeld. A cost effective
19 absorption chiller with plate heat exchangers using water and hydroxides, Applied
20 Thermal Engineering, 18 (2) (1998) 413-425.
- 21 [6] W. A., Ryan. Water absorption in an adiabatic spray of aqueous lithium bromide
22 solution. AES - Vol. 31, International Absorption Heat Pump Conference, ASME
23 155-162.

- 1 [7] V. E. Nakoryakov, N. I. Grigoreva. Combined heat and mass transfer during
2 absorption in drops and films. *Journal of Engineering Physics*, 32 (3) (1977) 243-
3 247.
- 4 [8] I. Morioka, M. Kiyota, A. Ousaka, T. Kobayashi. Analysis of steam absorption by
5 a subcooled droplet of aqueous solution of LiBr, *JSME International Journal*,
6 Series II, 35 (3) (1992) 458-464.
- 7 [9] M. Venegas, M. Izquierdo, P. Rodríguez, A. Lecuona. Heat and mass transfer
8 during absorption of ammonia vapour by $\text{LiNO}_3\text{-NH}_3$ solution droplets,
9 *International Journal of Heat and Mass Transfer*, 47 (2004) 2653-2667.
- 10 [10] M. Venegas, P. Rodríguez, A. Lecuona, M. Izquierdo. Spray absorbers in
11 absorption Systems using lithium nitrate-ammonia solution, *International Journal*
12 *of Refrigeration*, 28 (2005) 554-564.
- 13 [11] F. S. K. Wanakulasuriya, W. M. Worek. Adiabatic water absorption properties of
14 an aqueous absorbent at very low pressures in a spray absorber. *International*
15 *Journal of Heat and Mass Transfer*, 49 (2006) 1592-1602.
- 16 [12] A. Lecuona, R. Ventas, M. Venegas, A. Zacarías, R. Salgado. Optimum hot water
17 temperature for absorption solar cooling. *Solar Energy* 83 (10) (2009) 1806-1814.
- 18 [13] R. Best, L. Porras, F. A. Holland. Thermodynamic design for absorption heat
19 pump systems operating on ammonia-lithium nitrate-Part one: Cooling. *Heat*
20 *Recovery Systems & CPH* 11 (1) (1991) 49-61.
- 21 [14] R. Best, L. Porras, I. Pilatowsky F. A. Holland. Thermodynamic design for
22 absorption heat pump systems operating on ammonia-lithium nitrate -Part two:
23 Heating. *Heat Recovery Systems & CPH* 11 (2/3) (1991) 103-111.

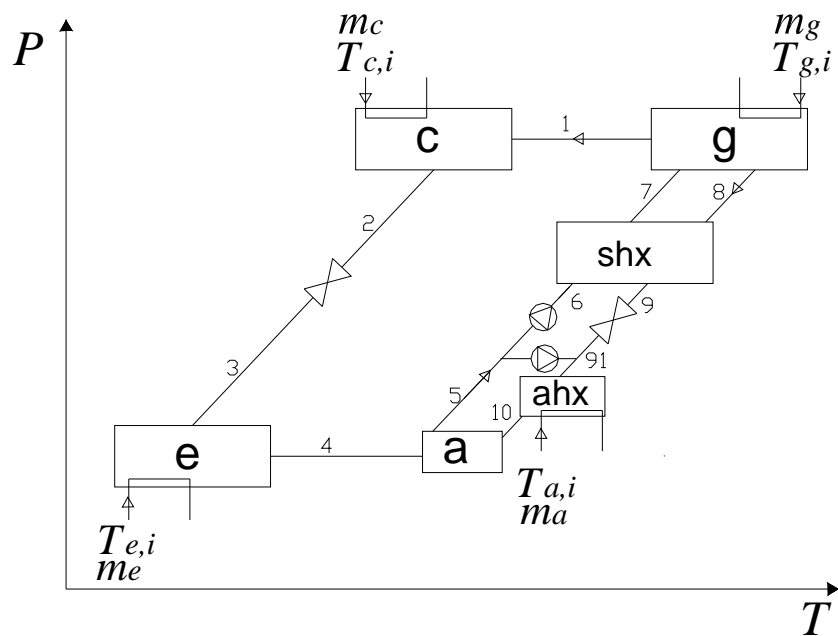
- 1 [15] R. Ayala, C. L. Heard, F. A. Holland. Ammonia/lithium nitrate
2 absorption/compression refrigeration cycle. Part I. Simulation. Applied Thermal
3 Engineering 17 (3) (1997) 223-233.
- 4 [16] D. W. Sun. Comparison of the performance of $\text{NH}_3\text{-H}_2\text{O}$, $\text{NH}_3\text{-LiNO}_3$ and $\text{NH}_3\text{-}$
5 NaSCN absorption refrigeration systems. Energy Conversion and Management 39
6 (5/6) (1998) 357-368.
- 7 [17] C.A. Infante Ferreira, Operating characteristics of $\text{NH}_3\text{-LiNO}_3$ and $\text{NH}_3\text{-NaSCN}$
8 absorption refrigeration machines, 19th Int. Congress of Refrigeration, Proceeding
9 Volume III, 1995.
- 10 [18] R. Ventas, A. Lecuona, A. Zacarías, M. Venegas. Ammonia-lithium nitrate
11 absorption chiller with an integrated low-compression booster cycle for low
12 driving temperatures. Applied Thermal Engineering, 30 (2010), pp. 1351-1359.
- 13 [19] A. B. Newman. The drying of porous solids: diffusion and surface emission
14 equations. Trans. AIChE 27 (1931), pp. 203-220.
- 15 [20] T. Elperin, A. Fominykh, Z. Orenbakh. Coupled heat and mass transfer during
16 nonisothermal absorption by falling droplet with internal circulation. Int. J. of
17 Refr. 30 (2007) pp. 274-281.
- 18 [21] Z. Feng, E. E. Michaelides. Int. J. Heat & Mass Trans. (2001) 44 pp. 4445-4454.
19 Heat and mass transfer coefficients of viscous spheres.
- 20 [22] H. Lu, T. Wu, Y. Yang, J. Ma. Transient heat and mass transfer in a drop
21 experiencing absorption with internal circulation. Int. Comm. in Heat and Mass
22 Transfer. 25, 8, November 1998, pp. 1115-1126.
- 23 [23] R. Krönig, J C. Brink, On the theory of extraction from falling droplets. Appl.
24 Scient. Res. A2, 142 (1951). Springer Netherlands.

- 1 [24] Acosta-Iborra, A., García, N., Santana, D., 2009. Modelling non-isothermal
2 absorption of vapour into expanding liquid sheets. *International Journal of Heat*
3 *and Mass Transfer*, 52, pp. 3042-3054.
- 4 [25] S. A. Klein, F. Alvarado. *Engineering Equation Solver*, v. 8.186-3D, F-Chart
5 Software, Middleton, WI, 1999.
- 6 [26] A. Zacarías. *Transferencia de masa y de calor en absorbedores adiabáticos con*
7 *aplicación de la disolución amoniaco-nitrato de litio*, PhD Thesis, Universidad
8 Carlos III de Madrid, Spain, <http://hdl.handle.net/10016/5635>.

- 1 Figure 1. Layout of the single-effect absorption cycle with the adiabatic absorber.
- 2 Figure 2. Layout of the single-effect absorption cycle with a diabatic absorber, showing
3 the optional recirculation circuit.
- 4 Figure 3. Coefficient of performance COP versus recirculation ratio rr for different
5 approach to equilibrium factors, $F_{ad} = \{0.5, 0.6, 0.7, 0.8, 0.9, 1.0\}$ and $T_{g,i} = 85\text{ }^\circ\text{C}$, for
6 the adiabatic absorber.
- 7 Figure 4. Cooling capacity \dot{Q}_e versus recirculation ratio rr for different approach to
8 equilibrium factors, $F_{ad} = \{0.5, 0.6, 0.7, 0.8, 0.9, 1.0\}$ and $T_{g,i} = 85\text{ }^\circ\text{C}$, for the adiabatic
9 absorber. Figure 5 Equivalent approach factor to diabatic equilibrium F_d and approach
10 factor to maximum ammonia mass fraction diabatic equilibrium $F_{d,max}$ versus
11 recirculation ratio rr for different approach factors to adiabatic equilibrium $F_{ad} = \{0.5,$
12 $0.6, 0.7, 0.8, 0.9, 1.0\}$ and $T_{g,i} = 85\text{ }^\circ\text{C}$ for the adiabatic absorber.
- 13 Figure 6. Coefficient of performance COP versus driving inlet temperature $T_{g,i}$ for
14 different recirculation ratios, $rr = \{0, 2, 4, 6, 8\}$, using $F_{ad} = 1$ for the adiabatic
15 absorber. The COP of the equivalent diabatic absorber is depicted as a reference.
- 16 Figure 7. Cooling capacity \dot{Q}_e versus driving inlet temperature $T_{g,i}$ for different
17 recirculation ratios, $rr = \{0, 2, 4, 6, 8\}$ and $F_{ad} = 1$ for the adiabatic absorber. The
18 cooling capacity of the equivalent diabatic absorber is depicted as a reference.
- 19 Figure 8. Approach factor to diabatic equilibrium F_d and approach factor to maximum
20 ammonia mass fraction diabatic equilibrium $F_{d,max}$ versus driving inlet temperature $T_{g,i}$
21 for different recirculation ratios, $rr = \{0, 2, 4, 6, 8\}$ and $F_{ad} = 1$, for the adiabatic
22 absorber. $F_{d,max}$ versus driving inlet temperature $T_{g,i}$.

- 1 Figure 9. Diabatic approach to equilibrium factor F_d versus driving inlet temperature $T_{g,i}$
- 2 for different absorber heat exchanger conductances, $UA_{ahx} = \{2,250; 3,000; 3,750;$
- 3 $4,500; 5,250\} \text{W m}^{-2} \text{K}^{-1}$, $F_{ad} = 1$ and $rr = 8$, for the adiabatic absorber.
- 4 Table 1. Constant input variables for the simulation.
- 5 Table 2. Enthalpy, temperature and concentrations at the inlet and outlet of the absorber
- 6 for $T_{g,i} = 85 \text{ }^\circ\text{C}$ and $F_{ad} = 1$.

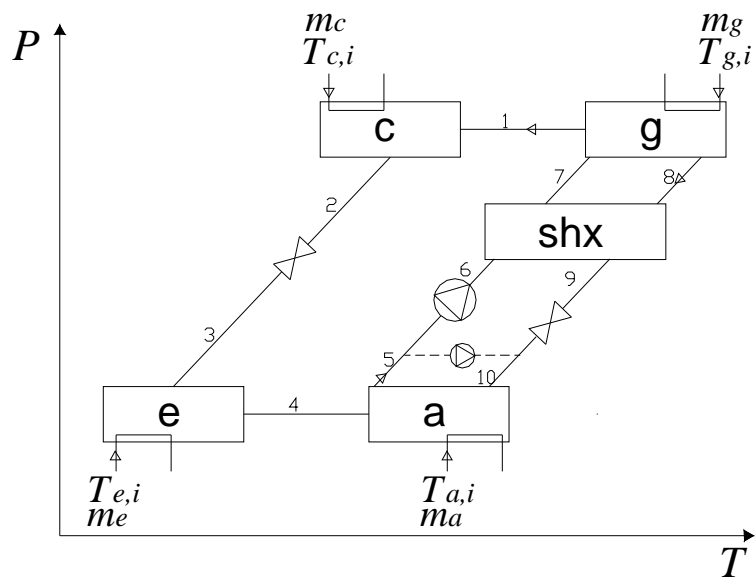
ACCEPTED MANUSCRIPT



1
2

3 Figure 1. Layout of the single-effect absorption cycle with the adiabatic absorber.

ACCEPTED MANUSCRIPT



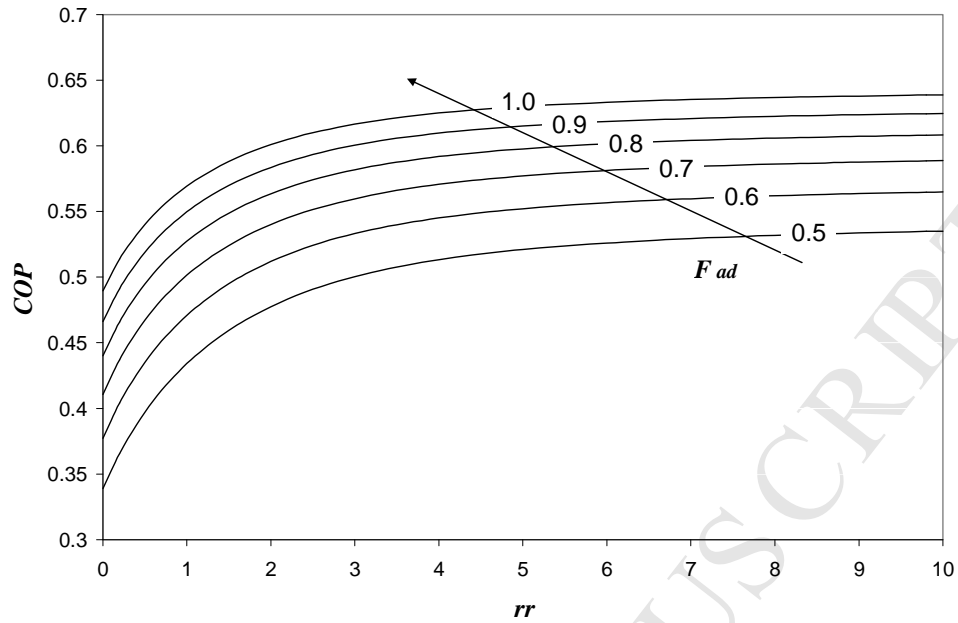
1

2 Figure 2. Layout of the single-effect absorption cycle with a diabatic absorber, showing

3

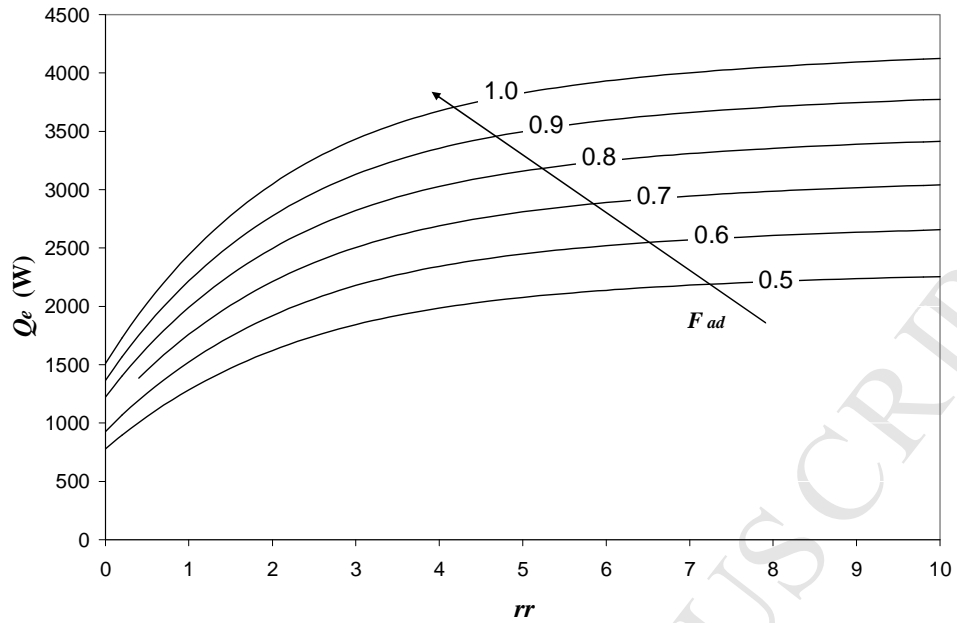
the optional recirculation circuit.

ACCEPTED MANUSCRIPT



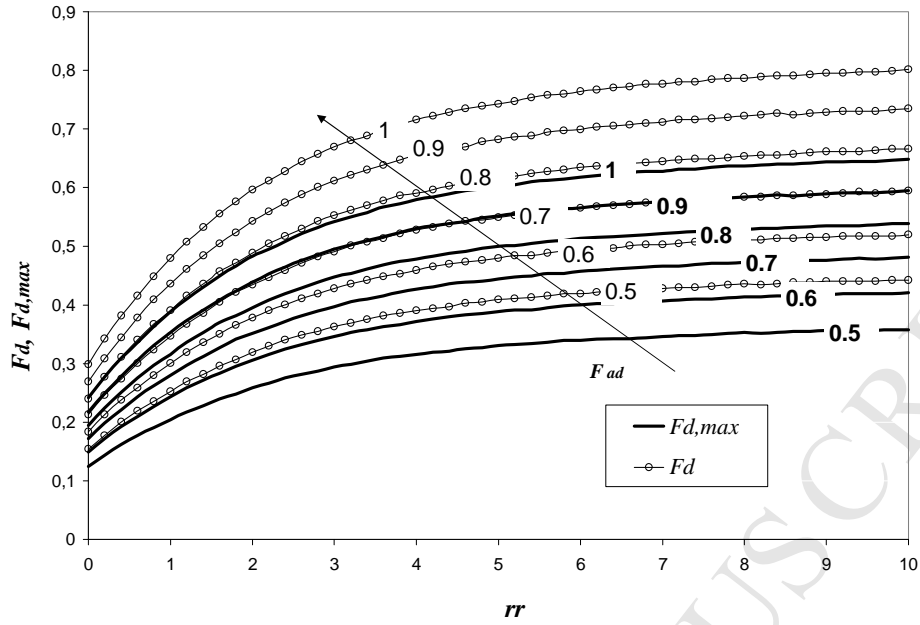
1

2 Figure 3. Coefficient of performance COP versus recirculation ratio rr for different
3 approach to equilibrium factors, $F_{ad} = \{0.5, 0.6, 0.7, 0.8, 0.9, 1.0\}$ and $T_{g,i} = 85\text{ }^\circ\text{C}$, for
4 the adiabatic absorber.



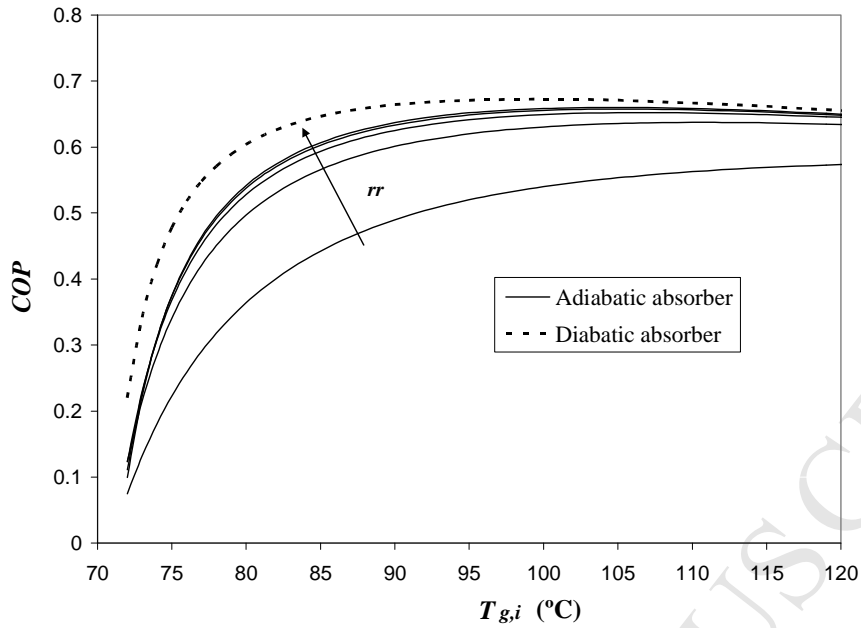
1

2 Figure 4. Cooling capacity \dot{Q}_e versus recirculation ratio rr for different approach to
 3 equilibrium factors, $F_{ad} = \{0.5, 0.6, 0.7, 0.8, 0.9, 1.0\}$ and $T_{g,i} = 85\text{ }^\circ\text{C}$, for the adiabatic
 4 absorber.



1

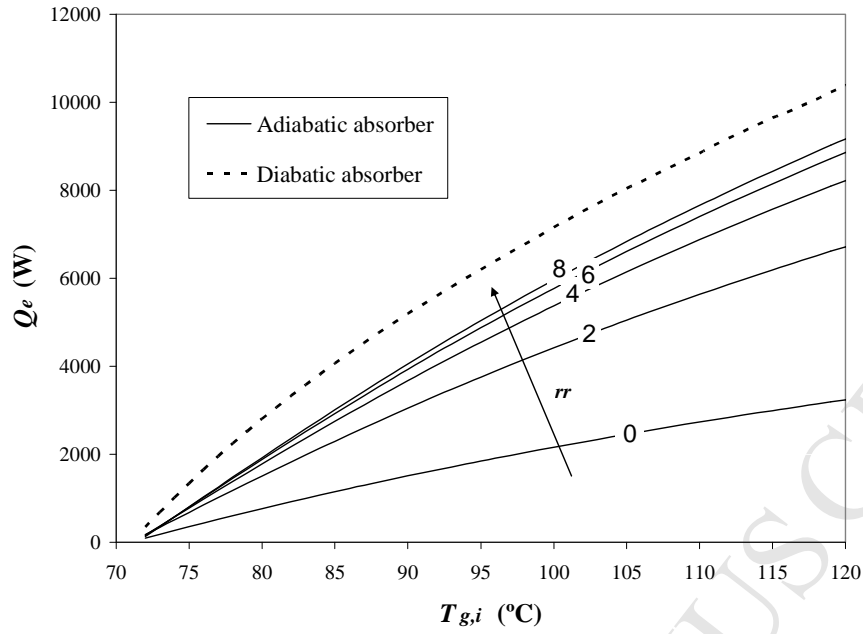
2 Figure 5. Equivalent approach factor to diabolic equilibrium F_d and approach factor to
 3 maximum ammonia mass fraction diabolic equilibrium $F_{d,max}$ versus recirculation ratio
 4 rr for different approach factors to adiabatic equilibrium $F_{ad} = \{0.5, 0.6, 0.7, 0.8, 0.9,$
 5 $1.0\}$ and $T_{g,i} = 85\text{ }^\circ\text{C}$ for the adiabatic absorber.



1

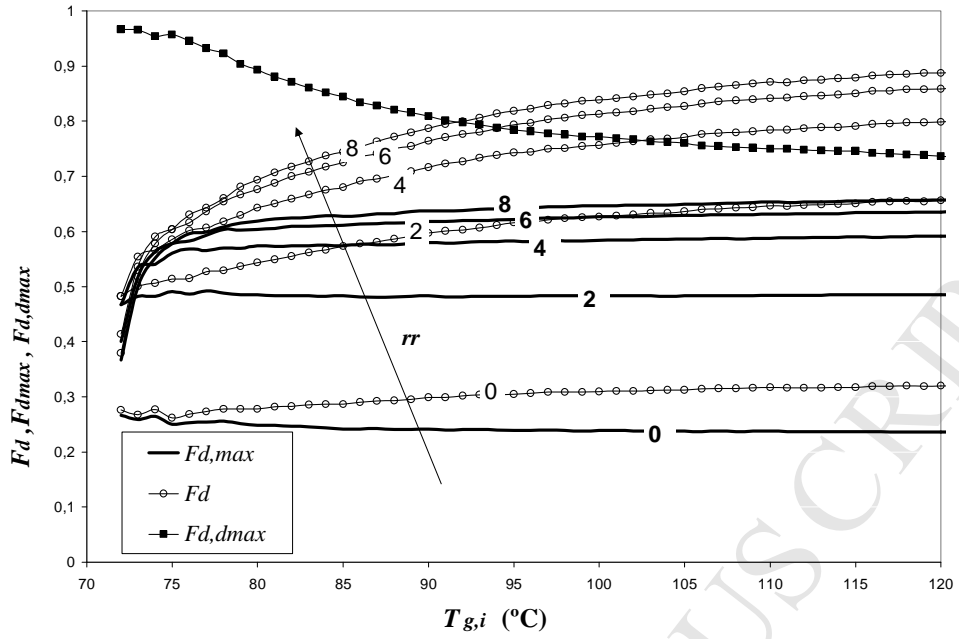
2 Figure 6. Coefficient of performance COP versus driving inlet temperature $T_{g,i}$ for
 3 different recirculation ratios, $rr = \{0, 2, 4, 6, 8\}$, using $F_{ad} = 1$ for the adiabatic
 4 absorber. The COP of the equivalent diabatic absorber is depicted as a reference.

ACCEPTED MANUSCRIPT



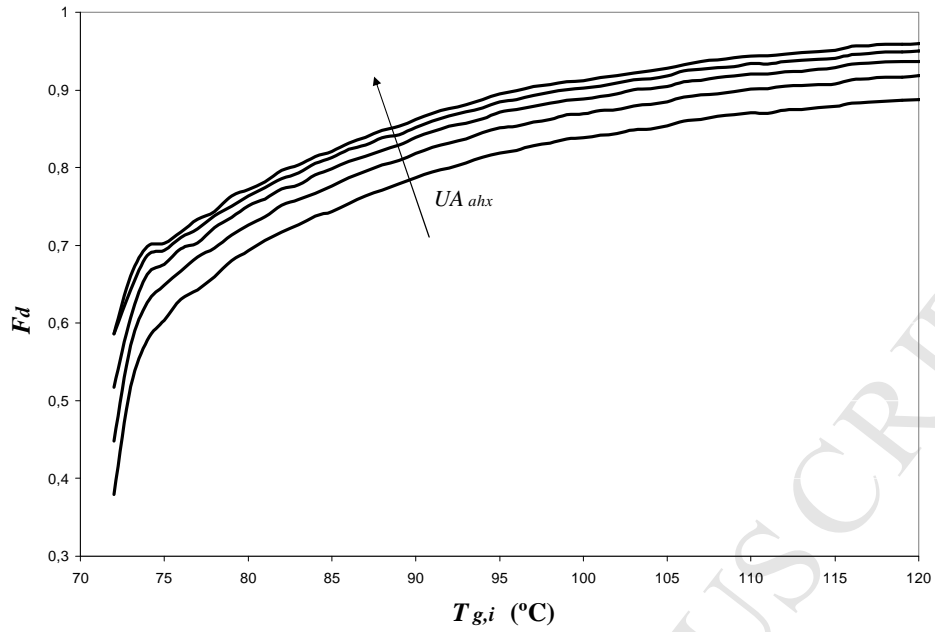
1

2 Figure 7. Cooling capacity \dot{Q}_e versus driving inlet temperature $T_{g,i}$ for different
 3 recirculation ratios, $rr = \{0, 2, 4, 6, 8\}$ and $F_{ad} = 1$ for the adiabatic absorber. The
 4 cooling capacity of the equivalent diabatic absorber is depicted as a reference.



1

2 Figure 8. Approach factor to diabatic equilibrium F_d and approach factor to maximum
 3 ammonia mass fraction diabatic equilibrium $F_{d,max}$ versus driving inlet temperature $T_{g,i}$
 4 for different recirculation ratios, $rr = \{0, 2, 4, 6, 8\}$ and $F_{ad} = 1$, for the adiabatic
 5 absorber. $F_{d,dmax}$ versus driving inlet temperature $T_{g,i}$.



1

2 Figure 9. Diabatic approach to equilibrium factor F_d versus driving inlet temperature $T_{g,i}$
 3 for different absorber heat exchanger conductances, $UA_{ahx} = \{2,250; 3,000; 3,750;$
 4 $4,500; 5,250\} \text{W m}^{-2} \text{K}^{-1}$, $F_{ad} = 1$ and $rr = 8$, for the adiabatic absorber.

1

Input Variable	Value	Input Variable	Value
η_{hb}	0.5	A_c	1.8 m ²
η_{mb}	0.5	A_e	1.0 m ²
\dot{m}_a	0.35 kg s ⁻¹	A_g	0.9 m ²
\dot{m}_c	0.35 kg s ⁻¹	A_{shx}	0.7 m ²
\dot{m}_e	0.4 kg s ⁻¹	UA_a	2.25·10 ³ W K ⁻¹
\dot{m}_g	0.15 kg s ⁻¹	$U_{c,col}$	200 W m ⁻² K ⁻¹
\dot{m}_6	0.05 kg s ⁻¹	$U_{c,tp}$	1.8·10 ³ W m ⁻² K ⁻¹
$T_{a,i}$	30 °C	$U_{c,sub}$	1.0·10 ³ W m ⁻² K ⁻¹
$T_{c,i}$	30 °C	$U_{e,tp}$	2.5·10 ³ W m ⁻² K ⁻¹
$T_{e,i}$	8 °C	$U_{e,sup}$	200 W m ⁻² K ⁻¹
T_c	39 °C	$U_{g,bo} = U_{shx,bo}$	2.0·10 ³ W m ⁻² K ⁻¹
T_e	0 °C	$U_g = U_{shx}$	1.5·10 ³ W m ⁻² K ⁻¹

2

3 Table 1. Constant input variables for the simulation.

1

Variable	Adiabatic absorber $rr = 0$	Adiabatic absorber $rr = 6$	Equivalent diabatic absorber
h_5 (kJ kg ⁻¹)	104.8	90.1	81.97
h_{10} (kJ kg ⁻¹)	76.5	79.8	97.59
T_5 (°C)	39.05	34.75	31.9
T_{10} (°C)	30.01	31.46	37.22
X_5	0.4897	0.5129	0.5276
X_8	0.4793	0.4866	0.4913
X_{10}	0.4793	0.5093	0.4913
$\Delta X = X_5 - X_8$	0.0104	0.0263	0.0363

2

3 Table 2. Enthalpy, temperature and concentrations at the inlet and outlet of the absorber

4 for $T_{g,i} = 85$ °C and $F_{ad} = 1$.

5